05,12

Control of bistability of two uniaxial spin transfer oscillators with field coupling and RLC load

© P.V. Kuptsov

Saratov Branch, Kotel'nikov Institute of Radio Engineering and Electronics, Russian Academy of Sciences, Saratov, Russia

E-mail: kupav@mail.ru

Received April 17, 2023
Revised April 17, 2023
Accepted May 11, 2023

Two uniaxial spin transfer oscillators with field coupling and RLC loads are considered. This system can demonstrate synchronized as well as non-synchronized oscillations. There is an area of bistability in the parameter space where these two regimes coexist. The mechanism of the bistability control is suggested. It is shown that if the RLC circuits are tuned in such a way that after the start their currents slowly and monotonically decay from high negative magnitudes to zero the oscillators forget their initial states and arrive at the vicinities of their fixed points. It provides the controllable start of the oscillations so that the bistability is suppressed in favor of either synchronous or non-synchronous regimes.

Keywords: magnetic moment precession, coupled oscillators, dipole interaction, bistability, controllable initial conditions.

DOI: 10.21883/PSS.2023.06.56099.05H

1. Introduction

A spin-transfer oscillator — is a nanoscale device that consists of three layers: two ferromagnetic layers separated by an insulating layer of non-magnetic material, see Figure 1. The lower layer, called the pinned layer, is quite thick and therefore its magnetization **p** remains constant. The top layer is thin. It is called free because its magnetization **m** can vary. A current flows through these layers, the direction of which is shown in the figure by the current density vector **j**. In addition, an external magnetic field $\mathbf{h}_{\text{ext}}$ can be applied. The electrons first pass through a pinned layer of constant magnetization, causing the current to become spin polarized. When current enters the top free layer, its polarization is destroyed, but the layer magnetization vector **m** is processed due to the effect of spin moment transfer. This results in the generation of low-power microwave radiation. A more detailed description of the physics of this phenomenon can be found, for example, in [1,2].

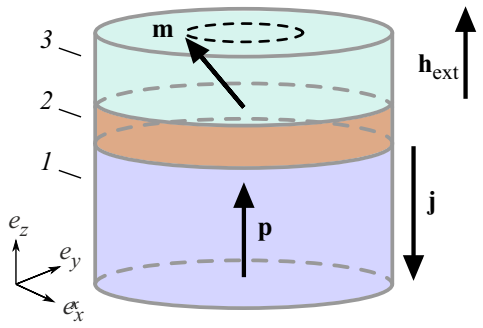

Figure 1. Design of a spin-transfer oscillator. The numbers indicate: *1* — pinned layer; *2* — insulating layer; *3* — free layer.

The first experimental observations of oscillations in spin-transfer oscillators were presented in papers [3,4]. The theoretical model of this oscillator is described by the Landau–Lifshitz–Gilbert–Slonczewski equation, which was first derived independently by Slonczewski [5] and Berger [6]. In dimensionless form, this equation is [1]:

$$\dot{\mathbf{m}} - \alpha\mathbf{m}\times\dot{\mathbf{m}} = -\mathbf{m}\times\mathbf{h}_{\text{eff}} + \frac{\beta}{1+c_p(\mathbf{m}\cdot\mathbf{p})}\,\mathbf{m}\times(\mathbf{m}\times\mathbf{p}). \tag{1}$$

Here „$\cdot$“ and „$\times$“ denote the scalar and vector products respectively; **m** — magnetization vector of the free layer normalized to one, $\|\mathbf{m}\| = 1$; **p** — also normalized to one constant layer magnetization, $\|\mathbf{p}\| = 1$; α — the Hilbert parameter responsible for precession attenuation; the β parameter is proportional to the current density value **j**. The effective magnetic field $\mathbf{h}_{\text{eff}}$ is equal to the sum of the external field, demagnetization and anisotropy fields (a more detailed description of this can be found in [1,7]).

We can assume that the free layer is a flat ellipsoid, the crystalline anisotropy is uniaxial, and the axis coincides with one of the axes of the ellipsoid. Note, that this simplification is physically relevant and quite often used, see for example the already mentioned work [1], and a number of others: [8–12]. In this case, the effective field can be written as follows:

$$\mathbf{h}_{\text{eff}} = \mathbf{h}_{\text{ext}} - \mathscr{D}\mathbf{m}, \tag{2}$$

where $\mathscr{D}$ — the diagonal tensor responsible for anisotropy and demagnetization and $\mathbf{h}_{\text{ext}}$ — the external field. The

coefficient c_p in equation (1) depends on the material properties of the oscillator and also on the degree of polarization acquired by the current in the pinned layer. It can take values in the range $-1 < c_p < 1$ [8]. In theoretical studies, it is often assumed to be zero, see e.g. [8–12]. We will also assume that $c_p = 0$. It is easy enough to check that for equation (1), the identity $\dot{\mathbf{m}} \cdot \mathbf{m} = 0$ holds, i. e. the norm of the vector $\mathbf{m}$ holds. We will always set the initial conditions as a unit vector, so $\|\mathbf{m}(t)\| = 1$ for any t.

In the general case, the system described by equation (1) has several selected directions: the current axis $\mathbf{j}$, the magnetization axis of the pinned layer $\mathbf{p}$, the external field axis $\mathbf{h}_{\text{ext}}$, the anisotropy and demagnetization related axes considered through the tensor $\mathscr{D}$. An interesting and physically feasible special case occurs when all these selected directions are oriented so that the system is symmetric about the axis z [1]. Then, the diagonal elements of the tensor $\mathscr{D}$ become $(0, 0, 1)$, the effective field takes the form $\mathbf{h}_{\text{eff}} = h_z \mathbf{e}_z - m_z \mathbf{e}_z$, where h_z — the only nonzero component of the external field along z, and equation (1) reduces to a much simpler form:

$$\dot{m}_x = m_z A m_x + B m_y,$$

$$\dot{m}_y = -B m_x + m_z A m_y,$$

$$\dot{m}_z = A(m_z^2 - 1),$$

$$A = \alpha \frac{m_z - h_z + \beta/\alpha}{1 + \alpha^2},$$

$$B = \frac{m_z - h_z - \beta\alpha}{1 + \alpha^2}. \tag{3}$$

Here m_x, m_y, m_z — components of vector $\mathbf{m}$.

This system of equations is explored in detail in the book [1]. It can be seen that it breaks down into two subsystems: the equation for m_z is independent of m_x and m_y. The equations for m_x and m_y are linear with respect to these variables. The non-trivial behavior arises because m_z is described by a cubic equation and enters the equations for m_x and m_y as a parameter.

The equation for m_z has three fixed points: $m_z = \pm 1$ and $m_z = h_z - \beta/\alpha$. One of them is always stable, and the other two unstable. For the condition $m_x^2 + m_y^2 + m_z^2 = 1$ at the stationary points $m_z = \pm 1$, the components m_x and m_y are zero, i.e. there is no oscillation. The conditions for their sustainability are as follows:

$$m_z = -1 \text{ stable at } h_z - \beta/\alpha < -1,$$

$$m_z = 1 \text{ stable at } h_z - \beta/\alpha > 1. \tag{4}$$

Fluctuations occur when the third fixed point is stable

$$m_z = h_z - \beta/\alpha \text{ stable at } -1 < h_z - \beta/\alpha < 1. \tag{5}$$

At this point, the solution to the system (3) is

$$m_x = \sqrt{1 - a^2}\cos(\omega t + f),$$

$$m_y = \sqrt{1 - a^2}\sin(\omega t + f), \quad m_z = a. \tag{6}$$

Here, f — an arbitrary initial phase, which depends on the choice of initial conditions and, due to axial symmetry, can be eliminated by rotating the oscillator about the axis z. The natural frequency ω and the stationary amplitude a are given by the formulas

$$\omega = \beta/\alpha, \tag{7}$$

$$a = h_z - \beta/\alpha. \tag{8}$$

Note, that (6) — is an exact solution to the system of equations (3). It is purely sinusoidal, without harmonics, due to the fact that the subsystem for the vibrational variables m_x and m_y is linear.

When considering the interaction of spin-transfer oscillators, communication between them is usually introduced in two ways: either through a common current or through magnetic fields. In the first case, the oscillators are connected in series or parallel and their interaction is due to the fact that the resistance of each oscillator depends on the cosine of the angle between the magnetizations of the upper and lower layers $\cos\theta = (\mathbf{m} \cdot \mathbf{p})$ (giant magnetic resistance effect) [8,9,11,12].

In the present paper, we consider the second case, when the coupling between the oscillators is carried out via magnetic fields. If we consider the magnetic field in dipole approximation, the coupling term is added as a correction to the effective field $\mathbf{h}_{\text{eff}}$ proportional to the magnetization. In the case of two oscillators, the effective field (2) of the first oscillator takes the form

$$\mathbf{h}_{\text{eff},1} = \mathbf{h}_{\text{ext}} - \mathscr{D}\mathbf{m}_1 + \varepsilon \mathbf{m}_2. \tag{9}$$

The effective field of the second oscillator is written in the same way. As the field of a single oscillator is quite small, it is natural to assume that the coupling between the oscillators ε is also small.

This type of coupling has been studied in [13] experimentally and in [14,15] theoretically. The article [16] derives the amplitude equation for coupled spin-transfer oscillators and considers, among other things, field coupling.

The main interest in the study of coupled spin-transfer oscillators is the question of their synchronization conditions. This phenomenon is known to be typical of coupled oscillatory systems [17]. In the case of spin-transfer oscillators, apart from the fundamental interest in this phenomenon, there is an important application aspect: a single oscillator generates low-power radiation [18] and the obvious way to obtain higher power is to form an array of oscillators oscillating synchronously with minimal difference phase dispersion.

In papers [8,9], the synchronization effects of an array of oscillators coupled by a common current are analyzed. A multistability effect is described, where fully synchronous oscillations coexist with nonsynchronous modes: quasi-periodic or chaotic. Clustering and chimeric states in

an array of common-current oscillators are considered in [11,12].

In paper [19], a system of two field-coupled uniaxial spin-transfer oscillators has been considered in a situation where a direct current flows through each of them, assuming that the currents are independent of each other and constant. It has been shown that there is a range of coupling magnitudes between the oscillators, in which two modes of oscillation coexist: phase synchronization and non-synchronous oscillation. Analytical evaluations for the boundaries of the area of existence of these modes in the parameter space have been obtained, and the bistable parameter area has been numerically analyzed. A formula for the phase difference constant of the oscillators, set in their phase synchronization mode, is also derived. According to this formula, at the threshold of synchronous operation, the phase difference is $\pi/2$ and decreases with the coupling value increase. Note, that similar patterns of retardance behavior are observed in [20], which studies the synchronization of magnetic vortices in exchange-coupled ferromagnetic disks.

In this paper, we consider two uniaxial spin-transfer oscillators with field interaction when an RLC-chain is connected in parallel to each of them. Since the electrical resistance of the spin-transfer oscillator depends on the direction of the magnetization vector **m**, together with the RLC-chain, the oscillator forms an oscillating circuit with an active element. It will be shown that in such a system, as well as in the absence of RLC chains, bistability is possible. A way of controlling it will be proposed — by selecting the parameters of the RLC-chains and the initial capacitor voltages, it can be achieved that the oscillators always choose one of two coexisting solutions, either synchronous or non-synchronous.

2. Equations of spin-transfer oscillators with RLC-chains and field coupling

The spin-transfer oscillator has an electrical resistance r, which depends on the cosine of the angle between its magnetization vector **m** and the magnetization of the pinned layer [21].

$$r = \frac{r_{\mathrm{p}} + r_{\mathrm{ap}}}{2}\left(1 - (\mathbf{m}\cdot\mathbf{p})\left(\frac{r_{\mathrm{ap}} - r_{\mathrm{p}}}{r_{\mathrm{ap}} + r_{\mathrm{p}}}\right)\right). \qquad (10)$$

Here, r_{p} — the minimum resistance that the oscillator has when the vectors **m** and **p** are parallel, and r_{ap} — the maximum possible resistance that is achieved when these vectors are antiparallel.

Consider two spin-transfer oscillators, each with an RLC chain connected in parallel and the oscillators themselves placed next to each other and interacting by means of magnetic fields, Figure 2.

The equation for each of the circuits is

$$L_i C_i \Gamma^2 \ddot{U}_i + (R_i + r_i) C_i \Gamma \dot{U}_i + U_i - I_i r_i = 0, \qquad (11)$$

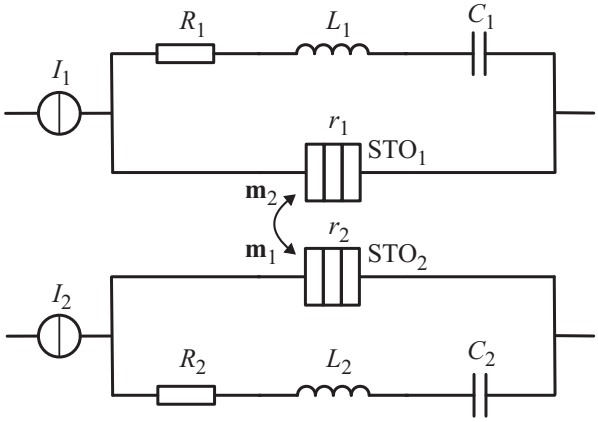

Figure 2. Schematic for incorporating two spin-transfer oscillators with RLC chains and interactions via magnetic fields.

where U_i — the capacitor voltage and Γ — the multiplier which is introduced to reconcile the circuit time and the renormalized spin-transfer oscillator time. It is convenient to rewrite this equation as a system of two equations for dimensionless voltage u_i and current w_i as follows:

$$\dot{u}_i = \chi_i w_i,$$

$$\dot{w}_i = \frac{\Omega_i^2}{\chi_i}\left((1 - \kappa_i m_{i,z})(1 - w_i) - u_i - \rho_i w_i\right). \qquad (12)$$

Here, it is taken into account that $(\mathbf{m}\cdot\mathbf{p}) = m_{i,z}$ due to $\mathbf{p} = (0, 0, 1)$. The following replacements have been made:

$$w_i = \frac{\dot{U}_i C_i \Gamma}{I_i}, \quad u_i = \frac{2U_i}{I_i(r_{i,\mathrm{ap}} + r_{i,\mathrm{p}})}, \quad \rho_i = \frac{2R_i}{r_{i,\mathrm{ap}} + r_{i,\mathrm{p}}},$$

$$\Omega_i = \frac{1}{\Gamma\sqrt{L_i C_i}}, \quad \chi_i = \frac{2}{C_i\Gamma(r_{i,\mathrm{ap}} + r_{i,\mathrm{p}})}, \quad \kappa_i = \frac{r_{i,\mathrm{ap}} - r_{i,\mathrm{p}}}{r_{i,\mathrm{ap}} + r_{i,\mathrm{p}}}. \qquad (13)$$

Note, that the dimensionless equations of a circuit with spin-transfer oscillators included in it are written in a similar way in [12].

Since in the dimensionless spin-transfer oscillator equation the parameter β is proportional to the current, the equation including the circuit connection is obtained from (3) by substituting $\beta \to \beta(1 - w)$. The terms responsible for the coupling between the oscillators remain the same as in the absence of a circuit. The corresponding formulas are the same as those derived in paper [19]. The result for the i-th oscillator associated with the oscillator j by field is

$$\dot{m}_{i,x} = m_{i,z} A_i m_{i,x} + B_i m_{i,y}$$

$$+ \frac{\varepsilon}{1 + \alpha_i^2}\left\{\alpha_i[m_{j,x} - (\mathbf{m}_i\cdot\mathbf{m}_j)m_{i,x}] - m_{i,y}m_{j,z} + m_{j,y}m_{i,z}\right\},$$

$$\dot{m}_{i,y} = -B_i m_{i,x} + m_{i,z} A_i m_{i,y}$$

$$+ \frac{\varepsilon}{1 + \alpha_i^2}\left\{\alpha_i[m_{j,y} - (\mathbf{m}_i\cdot\mathbf{m}_j)m_{i,y}] + m_{i,x}m_{j,z} - m_{j,x}m_{i,z}\right\},$$

$$\dot{m}_{i,z} = A_i(m_{i,z}^2 - 1)$$

$$+ \frac{\varepsilon}{1+\alpha_i^2}\{\alpha_i[m_{j,z} - (\mathbf{m}_i \cdot \mathbf{m}_j)m_{i,z}] - m_{i,x}m_{j,y} + m_{j,x}m_{i,y}\},$$

$$A_i = \alpha_i \frac{m_{i,z} - h_z + \beta_i(1-w_i)/\alpha_i}{1+\alpha_i^2},$$

$$B_i = \frac{m_{i,z} - h_z - \beta_i(1-w_i)\alpha_i}{1+\alpha_i^2}. \quad (14)$$

Here, $m_{i,x}$, $m_{i,y}$, $m_{i,z}$ — components of the vector $\mathbf{m}_i$, and the index j implies a different oscillator, i.e. when $i = 1$, we have to put $j = 2$ and vice versa.

3. Control of the coordinated start of oscillations in spin-transfer oscillators

The case of a system of two uniaxial field-coupled spin-transfer oscillators without RLC chains has been considered in detail in [19]. It is shown that at certain values of ε and β_i (coupling strength and natural frequencies, respectively) a full synchronization regime is possible. The oscillations occur in the xy plane, they are in-phase and the m_z components coincide with each other and remain constant. There is an area in parameter space in which a non-synchronous regime coexists with a synchronous regime. In this regime, the oscillator frequencies in the xy plane are close to the natural frequencies, and the m_z components oscillate with frequencies close to the difference of the natural frequencies.

To assess how the dynamics are affected by the connection of RLC chains, consider first one of the circuits (12), considering m_z as a constant parameter. This consideration makes sense because m_z always changes quite slowly.

The fixed point of this equation is

$$w = 0, \quad u = 1 - \kappa m_z, \quad (15)$$

and the eigenvalues can be found using the formula

$$\lambda_\pm = -\frac{\Omega}{2\chi}\left(\Omega(\rho - \kappa m_z + 1) \pm \sqrt{\Omega^2(\rho - \kappa m_z + 1)^2 - 4\chi^2}\right). \quad (16)$$

Since $m_z \le 1$, $\kappa < 1$, $\rho > 0$, $\chi > 0$, $\Omega > 0$, the expression $(\rho - \kappa m_z + 1)$ is always positive and there is always attenuation in the circuit. When the condition is met

$$\Omega(\rho - \kappa m_z + 1) < 2\chi \quad (17)$$

eigenvalues (16) form a complex conjugate pair with the negative real part $\mathrm{Re}\,\lambda = -\frac{\Omega}{2\chi}\left(\Omega(\rho - \kappa m_z + 1)\right)$. When

$$\Omega(\rho - \kappa m_z + 1) > 2\chi, \quad (18)$$

both eigenvalues are real and negative.

Consider first the case where inequality (17) holds. Set the parameters of the oscillators by equations (19),

$$\alpha = 0.001, \quad \beta_1 = 0.0055,$$

$$\beta_2 = 0.005, \quad \varepsilon = 0.0005, \quad h_z = 0, \quad (19)$$

and the parameters of the circuits — by formulas (20a). For ease of comparison, here are the other circuit parameter values, formulae (20b) and (20c), discussed below.

$$\rho = 1, \quad \Omega = 1.5, \quad \chi_{1,2} = 1, \quad \kappa = 0.3, \quad (20a)$$

$$\rho = 10, \ \Omega = 0.1, \ \chi_1 = 0.02, \ \chi_2 = 0.01, \ \kappa = 0.3, \quad (20b)$$

$$\rho = 10, \ \Omega = 0.1, \ \chi_1 = 0.01, \ \chi_2 = 0.02, \ \kappa = 0.3. \quad (20c)$$

It can be verified that with the chosen numerical values, condition (17) is fulfilled regardless of the value of m_z. The behavior of the system (12), (14) in this case is qualitatively similar to the case of no RLC-chains considered in [19]. In particularly, the system may exhibit bistability, where the type of solution depends on the choice of initial conditions.

The illustration is shown in Figure 3. Here in Figs. 3, *a, b, c* and *d* (panels on the left), the initial conditions for the oscillators are given by (21a), and in Figs. 3, *e, f, g* and it h (panels on the right) — by (21b),

$$\mathbf{v}_1 = (0.1, -0.1, 0.7), \quad \mathbf{v}_2 = (-0.2, 0.2, -0.7), \quad (21a)$$

$$\mathbf{v}_1 = (0.1, -0.1, -0.7), \quad \mathbf{v}_2 = (-0.2, 0.2, 0.7). \quad (21b)$$

It can be seen that in the first case, the components of the x oscillators synchronously oscillate with almost zero retardance, see Figure 3, *a*. Components y perform the same oscillations and are therefore not shown. The components z of the oscillators and the voltages and currents in the RLC circuits remain constant, see Figure 3, *b, c* and *d*. In the second case, the oscillators are out of sync, see Figure 3, *e*. In this case, the components z of the oscillators and the currents and voltages perform slow oscillations with small amplitude, Figure 3, *f, g* and *h*.

Consider now the case of real eigenvalues $\lambda_\pm$, i.e. when inequality (18) holds. The circuits parameters can be chosen such that λ_- has a large negative value. However, λ_+ can be a very small modulo negative value. This will cause the current through the RLC-chain to decay very slowly. In particularly, parameters (20b) and (20c) meet this condition regardless of m_z. The circuit currents appear in equations (14) as corrections to the parameters β_1 and β_2, on whose values the stability of the fixed points of the oscillators depends, see (4) and (5). This can be used to control the triggering of oscillations in spin-transfer oscillators.

The idea is to set the initial conditions for the RLC chains so that at the start w has a large negative value. This can be achieved by pre-charging the C_1 and C_2 capacitors to sufficiently high values. Then by discharging, they will give a high negative current in the circuit in the initial stages. As a consequence, the effective value of $\beta(1-w)$ will be shifted, and the fixed points of the $m_{1,2,z} = -1$ oscillators will become stable, see (4). Consequently, the oscillators will „forget“ their initial conditions, which may be arbitrary, and reach solutions $m_{1,2,x} = m_{1,2,y} = 0$, $m_{1,2,z} = -1$. The oscillators will manage to get sufficiently close to these

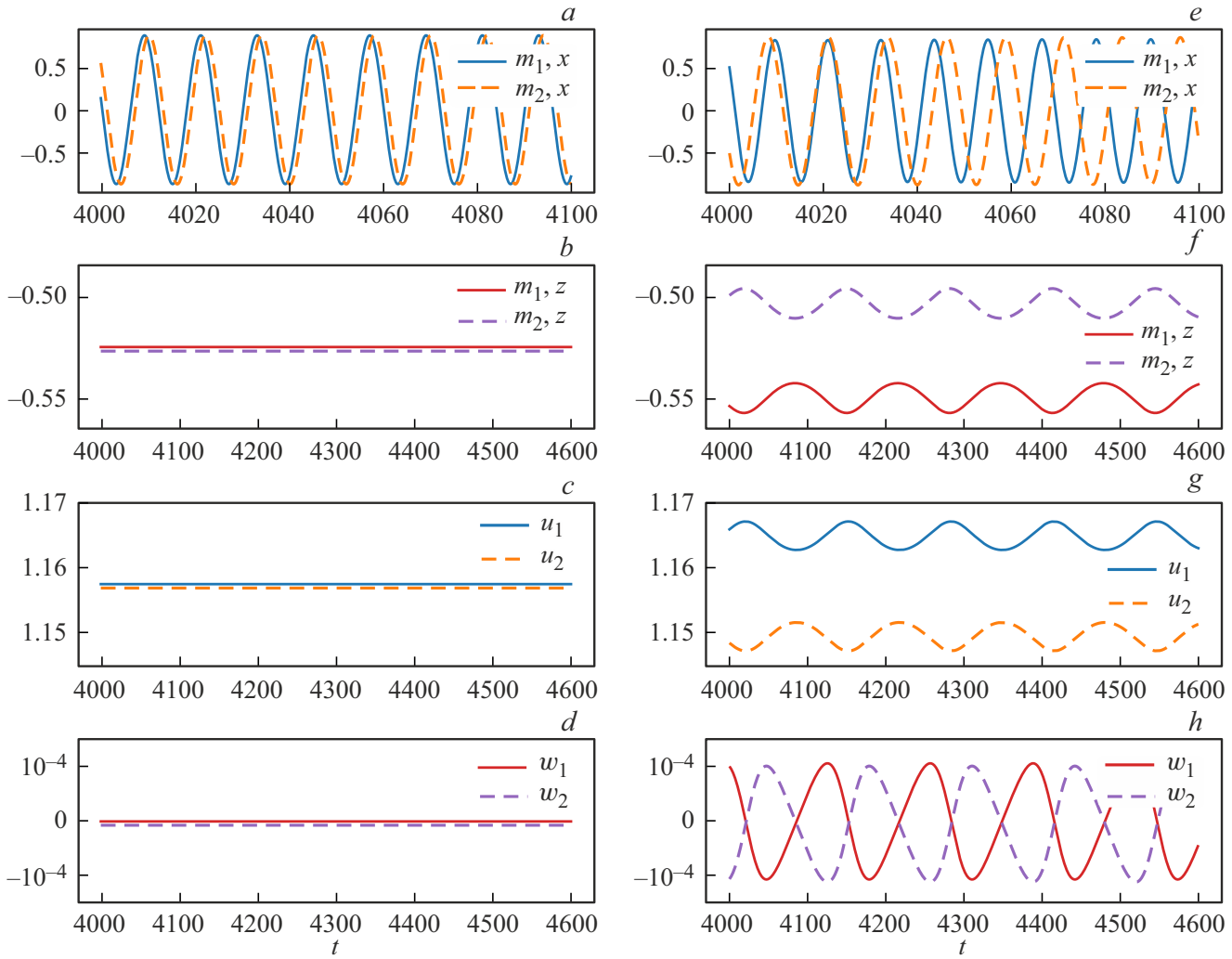

Figure 3. System bistability (12), (13): panels $(a) - (d)$ — synchronous, panels $(e) - (h)$ — non-synchronous. Solutions are obtained with the same parameters (19), (20a), but with different initial conditions. The initial conditions are taken as $\mathbf{m}_{1,2} = \mathbf{v}_{1,2}/\|\mathbf{v}_{1,2}\|$, where $\mathbf{v}_1$ and $\mathbf{v}_2$ for panels $(a) - (d)$ are given by equations (21a) and for $(e) - (h)$, — by equations (21b). The initial circuit currents and voltages are given as $w_1 = w_2 = 0$, $u_1 = 1.1$, $u_2 = 1.2$ in both cases, respectively.

solutions, provided that the attenuation in the RLC-chains is sufficiently small, which is what we are trying to achieve by selecting their parameters. When the current w becomes low enough, the fixed points on the poles become unstable again and the oscillators start to oscillate. It is essential, that it will always start with the same initial conditions. However, there is a subtle point. As has been shown in [19], the system's choice of one of the two solutions in the bistability regime depends on which of the initial values is greater, $m_{1,z}$ or $m_{2,z}$. Therefore, if the RLC circuits are identical, the oscillators will start to exit the fixed point almost simultaneously. This will again lead to bistability: the choice of solution will now depend on which of the two oscillators, due to random factors, started fluctuating slightly earlier than the other. To eliminate this, you need to make the RLC circuits slightly different. Then, one of the oscillators will always be slightly ahead of the other, eliminating uncertainty. This will lead to the absence of bistability.

The illustration is shown in Figure 4. The parameters in this figure are such that the solution does not depend on the choice of initial conditions. But for comparison, this figure is constructed with the same initial conditions for $\mathbf{m}_{1,2}$ as Figure 3. The starting currents are zero, $w_{1,2} = 0$, and the starting voltages are given as $u_{1,2} = 20 \pm 2\xi$, where $\xi \in (0, 1)$ —a random number, as in Figure 3. From Figure 4, *d* and *h*, it can be seen that this gives a sufficiently large negative initial current to force the oscillators to approach the fixed points $m_{1,2,z} = -1$, see Figure 4, *b* and *f*. Then, when the effective stability condition of these points is broken by the loss of currents $w_{1,2}$, the oscillation starts. Regardless of the initial conditions, the first oscillator always moves away from zero first. This ensures that the system is in the same, being synchronous in this example, mode

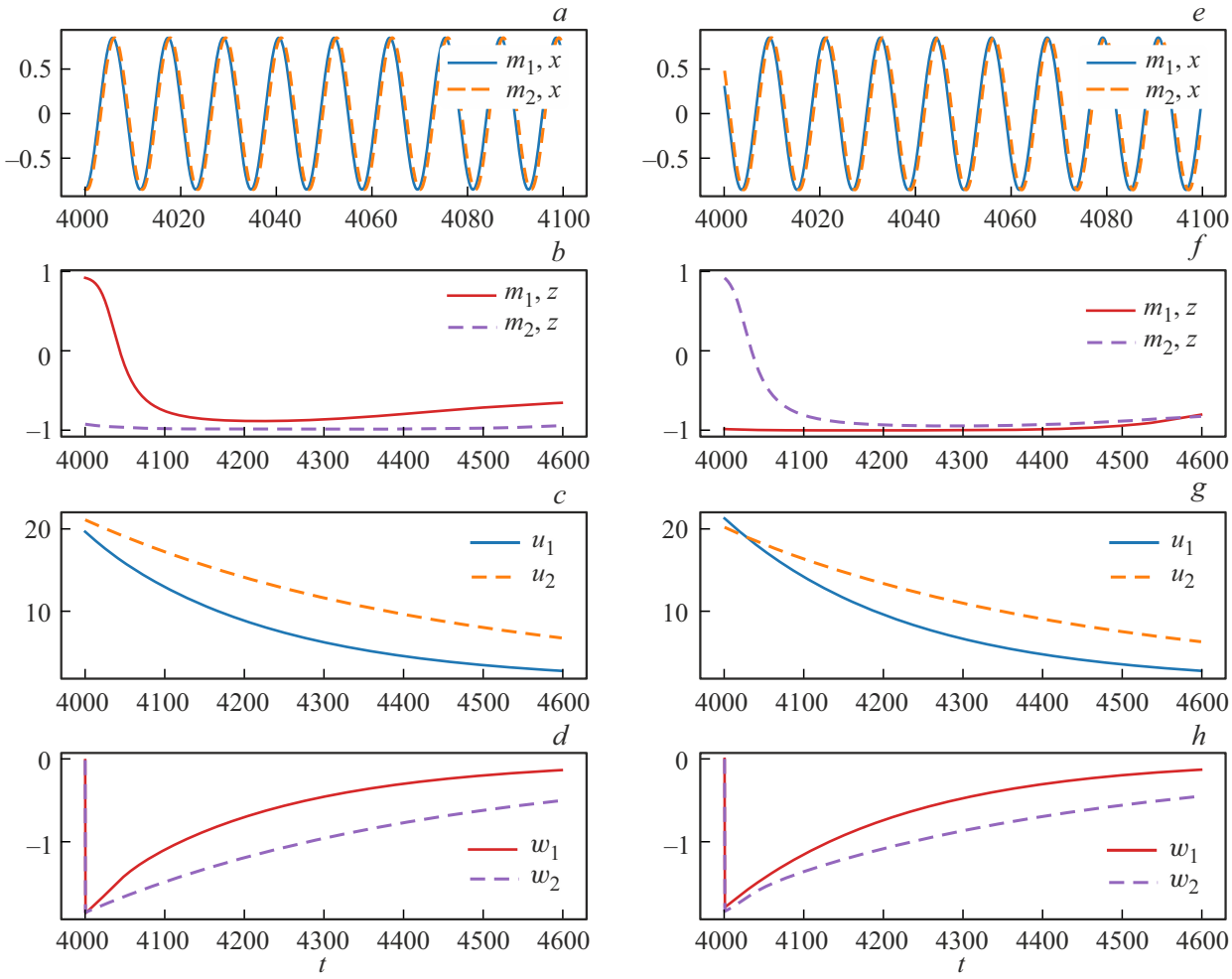

Figure 4. Bistability control in system (12), (14). The oscillator parameters are the same as in Figure 2, and for the RLC circuits, the parameters (20b) are given. The initial values for $\mathbf{m}_{1,2}$ are the same as in Figure 2. Initial circuit current values $w_{1,2} = 0$, initial voltage values $u_{1,2} = 20 \pm 2\xi$, where $\xi \in (0, 1)$ — a random number.

regardless of the initial conditions. In Figure 4, *a* and *e* we see synchronization in both cases.

To get a more complete picture, we will set the initial conditions randomly and calculate the relative frequency of occurrence of the synchronous solution P_{syn}. In our case, synchronization is conveniently identified by the spread of the $m_{1,2,z}$ component — in synchronous mode, it is zero. Figure 5 shows how P_{syn} depends on coupling strength for three different sets of RLC-chain parameters. The curve (*a*) corresponds to the case, where the RLC-chains have parameters (20a), i.e. an oscillating mode with fast damping takes place. This corresponds to Figure 3. There is no bistability control. When ε is small, all solutions are out of sync, but when ε is large enough, we always get synchronous solutions. The bistable area is roughly between $\varepsilon = 0.00025$ and $\varepsilon = 0.001$. Both types of solutions occur here, and the frequency of occurrence of synchronous solutions increases with increasing ε. If parameters (20b), which satisfy inequality (18), are involved, and in addition, one of the eigenvalues of the RLC-chain is very small and negative, the bistability disappears. As soon as ε enters an area where a synchronous solution exists, the system starts to always select only it. Parameter set (20c) differs from the previous set in that the values of χ_1 and χ_2 have been exchanged. This leads to that now $m_{2,z}$ always leaves the vicinity of the fixed point first. As can be seen in Figure 5, this also blocks bistability, but now as long as the non-synchronous solution is retained, the system always chooses it. Only switch to synchronous mode when the non-synchronous solution no longer exists.

Figure 6 shows the synchronous output frequency on the parameter plane (β_1, ε) using color shades. Figure 6, *a* is plotted for a set of parameters (20a) at which, there is no bistability control. We see here a dark blue language, within which the oscillators are synchronized. It is surrounded by lighter bistable — color saturation encodes the likelihood of synchronous mode P_{syn}. The white area below represents the unsynchronized oscillation mode. In Figure 6, *b*, the parameters (20b) are chosen to ensure that bistability is blocked. Recall that at these parameters, $m_{1,z}$ is the first

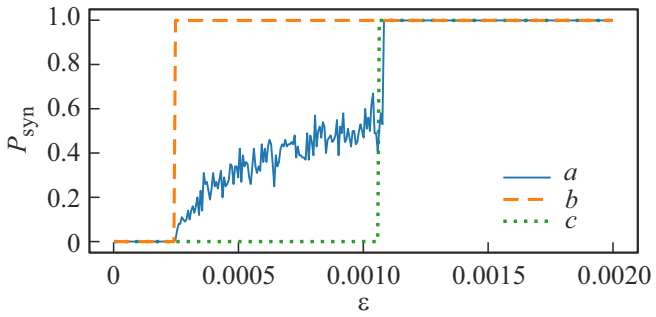

Figure 5. The relative frequency of obtaining a synchronous solution under randomly chosen initial conditions. The curve (a) is plotted for parameter values (20a) (RLC circuit with fast damping), and the curves (b) and (c) for (20b) and (20c) respectively (slow damping in the circuit). The oscillator parameters for all three cases are given by formulae (19) (with the obvious exception of ε, which varies along the horizontal axis).

to emerge from the fixed point. As can be seen from the figure, when $\beta_1 > \beta_2$, the bistability area is replaced by a synchronization area. If the opposite is true $\beta_1 < \beta_2$, an area of non-synchronous oscillation appears instead of bistability area. For parameters (20c), at which already $m_{2,z}$ exits the fixed point first, the situation is mirror-symmetric: to the left of β_1, the bistability area becomes the synchronization area and to the right — the unsynchronized oscillation area, Figure 6, *c*.

4. Conclusion

We have considered a system of two field-coupled spin-transfer oscillators, each with an RLC chain connected in parallel. Such a system can exhibit both fully synchronous and asynchronous oscillations. There is an are of parameters, in which there is bistability, when the two solutions

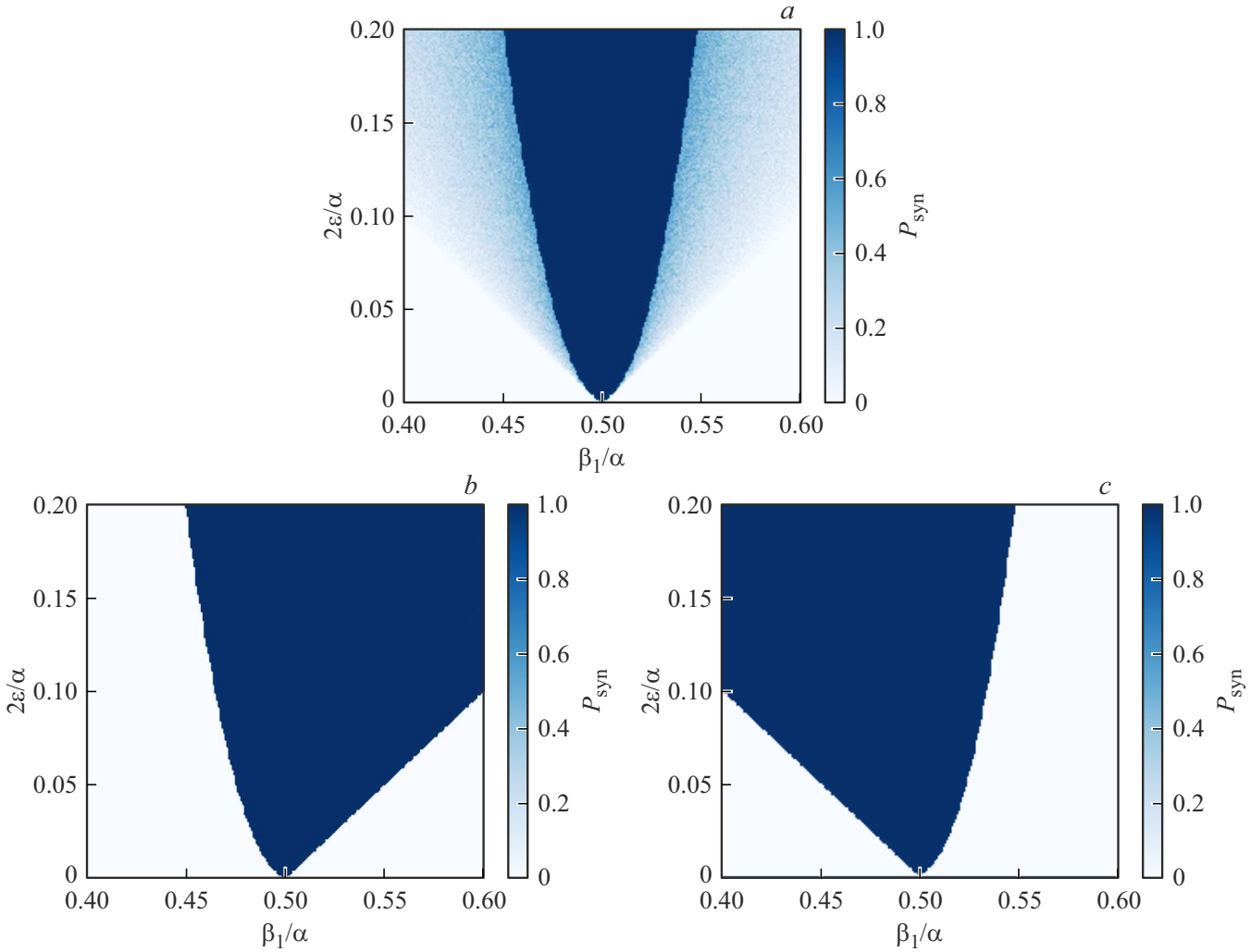

Figure 6. Relative frequency to obtain a synchronous solution with randomly chosen initial conditions on the parameter plane (β_1, ε). Panels (a), (b) and (c) are plotted for parameters (20a), (20b) and (20c), respectively. White represents a non-synchronous solution, dark blue — synchronization. Intermediate shades show bistability. The oscillator parameters, with the exception of the changing axes β_1 and ε, for all three cases are given by formulae (19), in particular $\beta_2/\alpha = 0.5$.

coexist. It is shown, that if one chooses the parameters of RLC-chains so that the current in them monotonically and slowly decreases from large negative values to zero, one can achieve „forgetting“ by spin-transfer oscillators of their arbitrary initial conditions. Controlled oscillation are triggered, allowing bistability to be suppressed in favor of both synchronous and non-synchronous modes.

Funding

The study was supported by a grant from the Russian Science Foundation No. 21-12-00121 https://rscf.ru/project/21-12-00121/https://rscf.ru/project/21-12-00121/

Conflict of interest

The author declares that he has no conflict of interest.

References

[1] I.D. Mayergoyz, G. Bertotti, C. Serpico. Nonlinear magnetization dynamics in nanosystems. Elsevier (2009). 466 p.
[2] Z. Zeng, G. Finocchio, H. Jiang. Nanoscale **5**, *6*, 2219 (2013).
[3] S.I. Kiselev, J.C. Sankey, I.N. Krivorotov, N.C. Emley, R.J. Schoelkopf, R.A. Buhrman, D.C. Ralph. Nature **425**, *6956*, 380 (2003).
[4] W.H. Rippard, M.R. Pufall, S. Kaka, S.E. Russek, T.J. Silva. Phys. Rev. Lett. **92**, 027201 (2004).
[5] J.C. Slonczewski. JMMM **159**, *1*, L1 (1996).
[6] L. Berger. Phys. Rev. B **54**, 9353 (1996).
[7] R. Skomski. Simple models of magnetism. Oxford University Press (2008). 336 p.
[8] D. Li, Y. Zhou, C. Zhou, B. Hu. Phys. Rev. B **82**, 140407 (2010).
[9] A. Pikovsky. Phys. Rev. E **88**, 032812 (2013).
[10] M.A. Zaks, A. Pikovsky. Physica D **335**, 33 (2016).
[11] M.A. Zaks, A. Pikovsky. Sci. Rep. **7**, *1*, 4648 (2017).
[12] M.A. Zaks, A. Pikovsky. Eur. Phys. J. B 92, 7, 160 (2019).
[13] S. Kaka, M.R. Pufall, W.H. Rippard, T.J. Silva, S.E. Russek, J.A. Katine. Nature **437**, *7057*, 389 (2005).
[14] S.M. Rezende, F.M. de Aguiar, R.L. Rodiguez-Suarez, A. Azevedo. Phys. Rev. Lett. **98**, 087202 (2007).
[15] M. Lakshmanan. Phil. Trans. Royal Soc. A **369**, *1939*, 1280 (2011).
[16] A. Slavin, V. Tiberkevich. IEEE Transact. Magn. **45**, *4*, 1875 (2009).
[17] A. Pikovsky, M. Rosenblum, J. Kurths. Synchronization. A universal concept in nonlinear sciences. Cambridge University Press (2002) 500 p.
[18] B. Georges, J. Grollier, M. Darques, V. Cros, C. Deranlot, B. Marcilhac, G. Faini, A. Fert. Phys. Rev. **101**, 017201 (2008).
[19] P.V. Kuptsov. Regular Chaotic Dynam. **27**, *6*, 697 (2022).
[20] D.A. Tatarsky, O.G. Udalov, A.A. Fraerman. ZHETF**163**, *3*, 366 (2023). (in Russian)
[21] J. Grollier, V. Cros, A. Fert. Phys. Rev. B **73**, 060409 (2006).

Translated by Ego Translating